nature portfolio

Peer Review File

Molecular insights into the activation mechanism of GPR156 in maintaining auditory function

Corresponding Author: Professor Renjie Chai

This file contains all reviewer reports in order by version, followed by all author rebuttals in order by version.

Attachments originally included by the reviewers as part of their assessment can be found at the end of this file.

Version 0:

Reviewer comments:

Reviewer #1

(Remarks to the Author)
In this manuscript, Ma et al. provide an elegant answer to the sustained role of GPR156 in maintaining auditory function. GPR156 is a unique class C GPCR which has a short N-terminal sequence, making it different from other known GPCRs of the same subfamily. Class C GPCRs are important drug targets for many diseases, because the complexity of their structure makes it extremely challenging to study the activation mechanism of these receptors. Starting from the actual biological significance (auditory function), this study cleverly combined in vivo experiments and structural biology experiments to reveal the structural characteristics of the special activation mechanism of GPR156, as well as the physiological significance of this activation mechanism in auditory function.

In summary, this manuscript is well-written and is easy to follow. The in vivo data, structural data, and functional data provided robust evidence to support its major findings. The proposed mechanism of the rapid and stable constitutive coupling to Gi3 protein and the dual functional role of the C-terminus is compelling and will be of interest to anyone focusing on class C GPCRs.

However, some minor revisions are required before acceptance for publication.

1. In the analysis of MD simulations, the simulation time is inconsistent. The simulation time for GPR156 (without lipid) is 300ns, while the GPR156 (with lipid) simulation time only lasts until 50ns (which can be seen in Supplementary Fig. 1). Although it is obvious that GPR156 (with lipid) is relatively stable, considering the rigor, it is necessary to keep the simulation time consistent. So please add this part of the data. In addition, there are two terms for the phospholipid-free GPR156 in figures, GPR156 (no lipid) in Extended Data Fig. 13g and GPR156 (without lipid) in Supplementary Fig. 1. Please keep the same name.

2. In statistical analysis, I only see the corresponding description of the in vitro functional experiment, and there is no clear description of statistical methods for the in vivo experiment related to mice. I think it is necessary to add this point.

3. Two kinds of AAV-mediated GPR156-shRNAs are mentioned in the manuscript, but no information about the corresponding shRNA is given. Therefore, the information of these shRNAs should be given in Extended Data Fig. 1 for follow-up by other readers.

4. In Fig. 5f and Extended Data Fig. 12c, the Cα of which amino acids were measured should be clearly written in the figure legend when the distance is given.

Reviewer #2

(Remarks to the Author)
The authors present the structure of a symmetric homodimer of GPR156 without bound G protein as well as another structure of the same dimer in complex with a Gi3 protein (stoichiometry 2:1). Both structures were obtained by cryo-EM.

Overall, the article is well written, allowing for a smooth reading experience for most readers.

Several structures of the GPR156 protein were published in the PDB earlier this year. These structures also describe a homodimer of GPR156 without a G protein or bound to a Go protein. However, as the authors mention in the discussion, these structures do not have the N-terminal and the C-terminal parts of the receptor, whose conformation explains certain functional properties. This article brings new insights into this particular receptor and also contributes to the broader understanding of class C GPCRs. The results presented are sufficiently novel for publication in Nature Communications.

The authors also conducted molecular dynamics simulations using state-of-the-art software and protocols (see remarks below). They use this modeling technique to evaluate the influence of the presence or absence of an endogenous ligand (phosphatidylglycerol) on the size of the transmembrane cavity. The authors conclude that in the absence of the ligand, the receptor conformation is no longer suitable for binding to a G protein due to a decrease in the volume of the cavity where the endogenous ligand binds.
However, the results and conclusion of this analysis can be explained by the application of an incorrect protocol during the preparation of the systems for the simulations. Additionally, the analysis mainly focuses on the extracellular region. Although a conformational change in the extracellular part is observed, the authors do not mention structural differences in the intracellular region that could prevent G protein binding. My comments on these points will be presented in the "Methodological Bias" section. I understand that the simulations represent only a small part of the article and that this does not change the general conclusions and the quality of the article. However, I feel obliged to request minor revisions before final publication in Nature Communications.
Nevertheless, it is possible that the preparation was done correctly, but this is not detailed in the Materials and Methods section. It will be necessary to provide additional details to include all necessary details on the simulation protocol. You will find my comments in the dedicated "Protocol Details" section.
Finally, the rest of my comments will be in the final section, "Miscellaneous", which includes various points for improvement.

##################
Methodological Bias
##################

Molecular Dynamics Simulations

The main problem I noted during the review of the protocol concerning molecular dynamics simulations is that the authors do not mention the use of constraints/restraints on the protein during the equilibration step. It is common, even necessary, to apply such constraints, as in these two articles (https://www.nature.com/articles/s41467-021-24438-5 and https://www.nature.com/articles/s41586-020-2469-4). The reason is that transmembrane cavities may not be solvated by CHARMM-GUI (between the lower and upper limits of the membrane plane). Consequently, the cavities are "filled" with vacuum (see figure). If no constraints are applied, the system is likely to collapse due to the vacuum. However, if constraints are applied to the protein, water molecules will populate the cavity. If the authors did not apply constraints during the equilibration phase, it will be necessary to rerun the simulations because the decrease in volume is probably due to the absence of water at the beginning of the simulation. Otherwise, it should be specified in the Materials and Methods section (see "Protocol Details" section). In any case, it will also be necessary to add a figure (Supplementary figure or extended data) showing structural deviation over time during the simulations to evaluate the stability of the systems.

Analysis of Cavity Volume

The authors measured the volume of the endogenous ligand binding site and showed a different conformation between the bound and unbound receptor. However, the authors infer that this would prevent G protein binding, without demonstrating a conformational change of the G protein binding site. The authors should provide additional evidence, such as measuring the volume of the intracellular cavity or a structural deviation such that steric hindrance prevents any G protein binding. That said, the duration of the simulations is probably not sufficient to potentially observe such a phenomenon. It is then possible to show the influence of the absence of the endogenous ligand on the dynamics of the helix ends in the intracellular region. If the intracellular part fluctuates more and significantly, then this is sufficient to conclude on an influence in the intracellular part preventing G protein binding.

##################
MD Protocol Details
##################

The protocol concerning the simulations is too briefly detailed. Some clarifications need to be added.
First, the authors refer to an article (reference 31: https://www.nature.com/articles/s41586-020-2469-4). Of course, it is common to refer to a previous publication for the Materials and Methods section. However, this can only be done if the publication comes from the same laboratory, which is not the case here. Moreover, the referenced publication does not provide more details, especially since the protocol does not seem exactly the same (e.g., different force field). Therefore, it is unclear which part is common and which is not.
I recommend adding the following elements to your protocol:
1. Structure Preparation: The structures presented in this article must undergo preparation before simulations (e.g., missing side chains). Please indicate how the structures were prepared. You should also specify which molecules were retained for the simulations (i.e., lipids).

2. Disulfide Bridge: In chain A of the apo structure (apo_GPR156-model.pdb), there is a disulfide bridge (C191 – C216) that is not present in chain B even though the sulfur atoms are close enough. Can you explain why? Did you consider disulfide bridges during the preparation of the structures for the simulations?
3. Model Construction: It is specified that the membrane model contains POPC and POPE (ratio 3:1) and that 7 CHL molecules are also present. Do these CHL molecules correspond to those initially present in the structure or were they added by CHARMM-GUI?
4. System Size: Indicate the dimensions and the number of atoms.
5. Type of Simulation: Specify that it is an all-atom simulation by classical molecular dynamics.

############
Miscellaneous
############

1. Line 198: You refer to Ballesteros-Weinstein numbering at this point in the article, but you use this notation earlier in the previous section. Please clarify the use of Ballesteros numbering when you use it for the first time (line 168).
2. Line 206: You write: "form van der Waals force", which is incorrect. You can simply indicate that residues L237, Y241, and L234 are in contact with residues M261 and N265.
3. Lines 253-254: You write: "a comparative analysis between apo GPR156 and the active GPR156 dimer revealed striking similarity (RMSD of 0.494 Å)". However, when I perform this alignment on alpha carbons, I get an RMSD of about 1 Å (apo_GPR156-model.pdb and GPR156_Gi3_complex-model.pdb). Did you consider all the residues of the protein or only part of it (i.e., the transmembrane domain)? Please clarify.
4. Figure 2, panel a: The text size of the legend of the phylogenetic tree (ion, orphan, amino acid, and sensory) is too small. I have to zoom in at 160% to read it. Please increase the font size.
5. Figure 4, panel e: The label size is too small as well.
6. Supplementary Figure 1: I noticed that the authors simulated the GPR156 homodimer with both endogenous ligands (phosphatidylglycerol). However, the duration is only 50 ns (1 replicate). Can you extend the simulations to 300 ns and 3 replicates? If not, it should be mentioned in the Materials and Methods section.

Reviewer #3

(Remarks to the Author)
Here Ma et al. present a significant study on the class C orphan G-protein-coupled receptor (GPCR) GPR156, emphasizing its role in auditory function via Gi2/3 signaling. The work presents the structural insights obtained from cryo-EM studies, which reveal an unconventional extracellular region and a dimerization interface that contributes to GPR156's activity. Furthermore, the authors describe a dual role of the C-terminus in G protein binding, offering mechanistic insights into how GPCR constitutive activity is sustained.

Overall, the work is very well presented, and both the functional and structural experiments are nicely done. While the aim of this research is highly significant, given the limited information available on the structural features of GPR156, the auditory function studies remain incomplete. To enhance the impact and comprehensiveness of this study, several clarifications are necessary.

Below are some suggestions:

1) Previous work by Kindt et al. (2021) demonstrated that GPR156 plays a crucial role in the development of the auditory system. In this study, the authors investigate whether GPR156 continues to be important after auditory maturity is reached. To address this, they performed in vivo knock-down experiments using AAV-mediated GPR156-shRNA at three time points: the auditory development stage (P2–P3), the mature auditory stage (P30), and the late stage of auditory maturation (P60). However, a significant issue is that the virus injections were carried out in the C57 mouse strain, which is known for early-onset hearing loss due to the Ahl allele, causing progressive hearing loss starting as early as 3 months of age. While the final time point in the study is P75, which is just under this threshold, it still presents potential challenges for interpreting the results. Both the downregulation of GPR156 and the mutation in cadherin 23 could contribute to the observed effects. The authors should address this limitation in their manuscript, discussing the implications of using the C57 strain for long-term auditory studies.

2) To ensure robust interpretation of the auditory function tests, it is essential to include both uninjected mice and mice injected with a control virus. These controls are particularly important given the use of the C57 strain, which has a predisposition for early-onset hearing loss. The authors only include ABR recordings from the contralateral ear as control. However, it is well-established that a virus injected in one ear can also affect hearing in the opposite ear."

3) In Figure 1, the authors show that both the P30 (Fig. 1a) and P60 (Fig. 1h) injections result in nearly 40% hair cell loss, although they do not distinguish between inner hair cells (IHCs) and outer hair cells (OHCs). It is intriguing that despite similar hair cell loss percentages, the P30 injection leads to a 10-20 dB SPL threshold elevation, while the P60 injection results in a 10-50 dB SPL elevation (Figs 1c and 1i). Additionally, given the significant hair cell loss observed in the representative immunofluorescence images, especially IHC loss in the cochlear base (Figs. 1e and 1k), it is surprising to see only a small ABR threshold elevation in the high-frequency region.

Therefore, it is important to count IHCs and OHCs separately. Furthermore, to assess the contribution of GPR156 to OHC

function, it would be informative to include DPOAE recordings. The discrepancy in threshold elevations (Figs 1c and 1i) should be further analyzed and better explained.

4) It is important to conduct immunohistochemistry assays using antibodies against GPR156 to quantify the reduction of the protein in hair cells and compare these results with the relative mRNA expression levels in the cochlea.

5) To strengthen the significance of GPR156 knockdown on auditory function, it is important to analyze the state of auditory innervation (afferent and efferent synapses) to the organ of Corti, as well as the condition of hair cell stereocilia. This can be accomplished through high-resolution immunofluorescence using well-described specific antibodies and subsequent analysis with a high-resolution confocal microscope.

6) In the present manuscript, the authors conduct an elegant study investigating the cryo-EM structures of human apo GPR156 and the GPR156–Gi3 complex, elucidating the structural features of the complex. The study is noteworthy for its thorough examination of the unique N-terminus, as well as the structural details of both the transmembrane domain (TMD) and C-terminus. Additionally, the authors assess basal activity through constructs with mutations in the C-terminal tail to analyze its interaction with the TMD of GPR156 and Gαi. However, the way it is written, avoiding explaining with details the performed experiments, coupled with the big amount of extended figures makes it difficult to follow. Simplifying the presentation of supplementary data and providing clearer explanations of the figures would enhance the readability and understanding of the study.

Version 1:

Reviewer comments:

Reviewer #1

(Remarks to the Author)
The authors have addressed my concerns.

Reviewer #2

(Remarks to the Author)
All the issues I previously highlighted have been addressed. The authors have done excellent work, and I believe the article is now ready for publication.

Reviewer #3

(Remarks to the Author)
The authors have carefully integrated my feedback, which has greatly enhanced the manuscript. I acknowledge their effort in effectively incorporating my recommendations, leading to a significant improvement in the overall quality of the work.

Responses to the reviewers' comments

We thank the reviewers for their constructive suggestions. We have carefully considered these comments in preparing the amendments and the changes are **highlighted** in the revised manuscript for clarity. We have copied each comment in **Black Bold**, followed by our own point-by-point response in Blue, including details about the corresponding changes to the manuscript in Red.

Response to Reviewer #1:

Reviewer #1:

In this manuscript, Ma et al. provide an elegant answer to the sustained role of GPR156 in maintaining auditory function. GPR156 is a unique class C GPCR which has a short N-terminal sequence, making it different from other known GPCRs of the same subfamily. Class C GPCRs are important drug targets for many diseases, because the complexity of their structure makes it extremely challenging to study the activation mechanism of these receptors. Starting from the actual biological significance (auditory function), this study cleverly combined in vivo experiments and structural biology experiments to reveal the structural characteristics of the special activation mechanism of GPR156, as well as the physiological significance of this activation mechanism in auditory function.

In summary, this manuscript is well-written and is easy to follow. The in vivo data, structural data, and functional data provided robust evidence to support its major findings. The proposed mechanism of the rapid and stable constitutive coupling to Gi3 protein and the dual functional role of the C-terminus is compelling and will be of interest to anyone focusing on class C GPCRs.

Response: We thank the Reviewer #1 for acknowledging the new insights provided in our manuscript and the high quality of the data.

However, some minor revisions are required before acceptance for publication.

Response: We thank and appreciate reviewer's comments for kindly providing some modifications to enhance our manuscript.

1. In the analysis of MD simulations, the simulation time is inconsistent. The simulation time for GPR156 (without lipid) is 300ns, while the GPR156 (with lipid) simulation time only lasts until 50ns (which can be seen in Supplementary Fig. 1). Although it is obvious that GPR156 (with lipid) is relatively stable, considering the rigor, it is necessary to keep the simulation time consistent. So please add this part of the data. In addition, there are two terms for the phospholipid-free GPR156 in figures, GPR156 (no lipid) in Extended Data Fig. 13g and GPR156 (without lipid) in Supplementary Fig. 1. Please keep the same name.

Response: We thank the reviewer for these kindly suggestions. We agree that the simulation time should be consistent between the GPR156 (without lipid) and the GPR156 (with lipid). We have therefore extended the simulation time of the GPR156 (with lipid) to 300 ns, and revised the following sentences and the corresponding analyses results, as listed below.

"Finally, to escape the uncertainties of the sampling results, three replicates of the production run of 300 ns MD simulation with different initial velocities were performed for both systems: the

GPR156 (with lipid) and the GPR156 (no lipid) (Supplementary Fig. 2). The stability of the two systems were evaluated by the RMSD of all the heavy atoms of the GPR156 dimer (Supplementary Fig. 1d)." (Lines 657-662)

The corresponding results in Extended Data Fig. 10h (Extended Data Fig. 13h in prior version) and Supplementary Fig. 2 (Supplementary Fig. 1 in prior version) have also been revised. Meanwhile, we have also revised the term for the phospholipid-free GPR156 in Supplementary Fig. 2 and replaced it with the term "GPR156 (no lipid)".

2. In statistical analysis, I only see the corresponding description of the in vitro functional experiment, and there is no clear description of statistical methods for the in vivo experiment related to mice. I think it is necessary to add this point.

Response: Thank you for your suggestions. According to your advice, we have added the description of statistical methods for the *in vivo* experiment related to mice in the Materials and methods section of statistical analysis, as listed below.

"Bar graphs depict the differences of each mutant relative to the WT receptor or contralateral ear/WT mice. *In vitro* data were from at least six independent experiments, each conducted in triplicate. *In vivo* experiments related to mice were repeated at least three times. $*P < 0.05$, $**P < 0.01$, $***P < 0.001$, $****P < 0.0001$ (two-tailed unpaired t test for all data)." (Lines 710-714)

3. Two kinds of AAV-mediated GPR156-shRNAs are mentioned in the manuscript, but no information about the corresponding shRNA is given. Therefore, the information of these shRNAs should be given in Extended Data Fig. 1 for follow-up by other readers.

Response: Thank you for your suggestions. According to your advice, we have added the information about the GPR156-shRNAs in the Materials and methods section of Plasmid design and AAV purification.

"The sense strand sequence of GPR156-shRNA1 and GPR156-shRNA2 were cgg agc atg caa tgt agc ttt and gta ccg ttt cta gtt cac aaa, respectively. And the loop sequence of GPR156-shRNA was tcaagag." (Lines 445-447)

4. In Fig. 5f and Extended Data Fig. 12c, the Cα of which amino acids were measured should be clearly written in the figure legend when the distance is given.

Response: We appreciate the reviewer for pointing out the problem. We have added these descriptions in our revised manuscript (Figure 5f and Extended Data Fig. 9c (previously Extended Data Fig. 12c)). We have also revised these figures for better presentation.

And these descriptions are shown below:

"Figure 5f, Upon G protein coupling, the dimeric TMD of five class C GPCRs (including $mGlu3_{free}$–$mGlu2_G$ (Cα of V699; PDB code: 8JD3), $mGlu4_{free}$–$mGlu2_G$ (Cα of V699; PDB code: 8JD5), $mGlu2_{free}$–$mGlu2_G$ (Cα of V769; PDB code: 7MTS), $CaSR_{free}$–$CaSR_G$ (Cα of M771; PDB code: 8WPU), and $GABA_{B1(free)}$–$GABA_{B2(G)}$ (Cα of C614; PDB code: 7EB2)) undergo conformational rearrangements, except for $GPR156_{free}$–$GPR156_G$." in Lines 1021-1026.

"Extended Data Fig. 9b, c, Statistical analysis of the dimeric interface area (**b**) and the distance (**c**) of class C GPCR dimers with the G protein (including $GPR156_{free}$–$GPR156_G$ (Cα of G244-

G244), $CaSR_{free}$–$CaSR_G$ (Cα of T828-A824; PDB code: 8WPU), $mGlu4_{free}$–$mGlu4_G$ (Cα of I804-I804; PDB code: 7E9H), $mGlu4_{free}$–$mGlu2_G$ (Cα of T808-V782; PDB code: 8JD5), $mGlu3_{free}$–$mGlu2_G$ (Cα of T792-V782; PDB code: 8JD3), $mGlu2_{free}$–$mGlu2_G$ (Cα of T783-V782; PDB code: 7MTS), and $GABA_{B1(free)}$–$GABA_{B2(G)}$ (Cα of A832-L712; PDB code: 7EB2)).” in Lines 1165-1171.

Response to Reviewer #2:

Reviewer #2:

The authors present the structure of a symmetric homodimer of GPR156 without bound G protein as well as another structure of the same dimer in complex with a Gi3 protein (stoichiometry 2:1). Both structures were obtained by cryo-EM.

Overall, the article is well written, allowing for a smooth reading experience for most readers.

Several structures of the GPR156 protein were published in the PDB earlier this year. These structures also describe a homodimer of GPR156 without a G protein or bound to a Go protein. However, as the authors mention in the discussion, these structures do not have the N-terminal and the C-terminal parts of the receptor, whose conformation explains certain functional properties. This article brings new insights into this particular receptor and also contributes to the broader understanding of class C GPCRs. The results presented are sufficiently novel for publication in Nature Communications.

The authors also conducted molecular dynamics simulations using state-of-the-art software and protocols (see remarks below). They use this modeling technique to evaluate the influence of the presence or absence of an endogenous ligand (phosphatidylglycerol) on the size of the transmembrane cavity. The authors conclude that in the absence of the ligand, the receptor conformation is no longer suitable for binding to a G protein due to a decrease in the volume of the cavity where the endogenous ligand binds.

However, the results and conclusion of this analysis can be explained by the application of an incorrect protocol during the preparation of the systems for the simulations. Additionally, the analysis mainly focuses on the extracellular region. Although a conformational change in the extracellular part is observed, the authors do not mention structural differences in the intracellular region that could prevent G protein binding. My comments on these points will be presented in the "Methodological Bias" section. I understand that the simulations represent only a small part of the article and that this does not change the general conclusions and the quality of the article. However, I feel obliged to request minor revisions before final publication in Nature Communications.

Nevertheless, it is possible that the preparation was done correctly, but this is not detailed in the Materials and Methods section. It will be necessary to provide additional details to include all necessary details on the simulation protocol. You will find my comments in the dedicated "Protocol Details" section.

Finally, the rest of my comments will be in the final section, "Miscellaneous", which includes various points for improvement.

Response: We thank the Reviewer #2 for this great suggestion. We have carefully read the suggestions listed below, and revised our manuscript.

##########

Methodological Bias

####################

 # Molecular Dynamics Simulations

The main problem I noted during the review of the protocol concerning molecular dynamics simulations is that the authors do not mention the use of constraints/restraints on the protein during the equilibration step. It is common, even necessary, to apply such constraints, as in these two articles (https://www.nature.com/articles/s41467-021-24438-5 and https://www.nature.com/articles/s41586-020-2469-4). The reason is that transmembrane cavities may not be solvated by CHARMM-GUI (between the lower and upper limits of the membrane plane). Consequently, the cavities are "filled" with vacuum (see figure). If no constraints are applied, the system is likely to collapse due to the vacuum. However, if constraints are applied to the protein, water molecules will populate the cavity. If the authors did not apply constraints during the equilibration phase, it will be necessary to rerun the simulations because the decrease in volume is probably due to the absence of water at the beginning of the simulation. Otherwise, it should be specified in the Materials and Methods section (see "Protocol Details" section). In any case, it will also be necessary to add a figure (Supplementary figure or extended data) showing structural deviation over time during the simulations to evaluate the stability of the systems.

Response: We thank the reviewer for these important suggestions. We have revised the method description of MD simulations to illustrate all necessary details in the "Material and Methods" section. In addition, the pre-equilibrium simulation result for the GPR156 (no lipid) system showed that the vacuum of the cavities has been filled with waters with the default restraint potential adopted on the GPR156, see the detail in Supplementary Fig. 1c. To address this import issue, we have revised the following sentences in the Materials and Methods section (listed below).

"After 5000 steps of energy minimization performed by the steepest descent algorithm, a 250 ps NVT equilibration simulation was performed at 310 K, with the default restraint potential ($k_{BC/SD/LIP/DIH}$=10.0/5.0/2.5/2.5 kcal·mol^{-1}·Å^{-2}) on the heavy atoms of backbone, sidechain, lipid and dihedral angle. Subsequently, a cumulatively 1.65 ns NPT equilibration to 1 atm was performed using the Berendsen barostat[62], with the restraint potential gradually reduced to zero." (Lines 647-652).

"During the pre-equilibrium simulation, the vacuum of the cavities of the transmembrane helices core for the GPR156 (no lipid) system was gradually filled with water molecules (Supplementary Fig. 1c)." (Lines 655-657).

In addition, we have also calculated the structural deviation over time for all the systems to evaluate the stability of the systems. The results were shown in Supplementary Fig. 1d.

 # Analysis of Cavity Volume

The authors measured the volume of the endogenous ligand binding site and showed a different conformation between the bound and unbound receptor. However, the authors infer that this would prevent G protein binding, without demonstrating a conformational

change of the G protein binding site. The authors should provide additional evidence, such as measuring the volume of the intracellular cavity or a structural deviation such that steric hindrance prevents any G protein binding. That said, the duration of the simulations is probably not sufficient to potentially observe such a phenomenon. It is then possible to show the influence of the absence of the endogenous ligand on the dynamics of the helix ends in the intracellular region. If the intracellular part fluctuates more and significantly, then this is sufficient to conclude on an influence in the intracellular part preventing G protein binding.

Response: We thank the reviewer for this important suggestion. To elucidate the influence of the absence of endogenous ligands on the dynamics of the helix ends in the intracellular region, we have measured the RMSD of the ends of TM3/5/6/7 and obtained a generally higher flexibility of the helix ends in GPR156 (no lipid) than GPR156 (with lipid), which could support the conclusion of the collapse of the cavities caused by the absence of endogenous ligands would prevent G protein binding. To address this issue, we have added and revised the following sentences.

"The increased RMSD values at the intracellular termini of the TM helix suggest that the depletion of the internal phospholipids hinders G protein binding (Supplementary Figs. 3-6, Supplementary Table 3)." (Lines 286-289).

"The RMSD of the transmembrane helices (TM3/5/6/7) ends (heavy atoms of 10 residues) in the intracellular side were calculated, and other C alpha atoms of the transmembrane helices were used for structural alignment (Supplementary Figs. 3-6; Supplementary Table 3). For the RMSD calculation, the first 10 ns was ignored and only the last 290 ns MD simulation data was used. GROMACS's rms function was used to calculate RMSD." (Lines 663-668).

####################

MD Protocol Details

####################

The protocol concerning the simulations is too briefly detailed. Some clarifications need to be added.

First, the authors refer to an article (reference 31: https://www.nature.com/articles/s41586-020-2469-4). Of course, it is common to refer to a previous publication for the Materials and Methods section. However, this can only be done if the publication comes from the same laboratory, which is not the case here. Moreover, the referenced publication does not provide more details, especially since the protocol does not seem exactly the same (e.g., different force field). Therefore, it is unclear which part is common and which is not.

Response: We thank the reviewer for these important suggestions. We have revised the method description of MD simulations to illustrate all necessary details in the "Material and Methods" section. And the MD simulation data (cleaned trajectories, start structure, simulation parameters) generated in this study have been deposited in the github (https://github.com/Yanzhang-ZJU/GPR156.git) and Zenodo (https://doi.org/10.5281/zenodo.13208133).

I recommend adding the following elements to your protocol:

1. Structure Preparation: The structures presented in this article must undergo preparation before simulations (e.g., missing side chains). Please indicate how the structures were prepared. You should also specify which molecules were retained for the simulations (i.e., lipids).

Response: We thank the reviewer for this important suggestion. We have revised the following sentences in the Materials and Methods section.

"From the apo structure of the GPR156 dimer complex, the two transmembrane helix core-bound phospholipids were removed, except the PGs (36:2) and the cholesterol molecule in the interface of GPR156 dimer. The retained GPR156-dimer complex was used as the input conformation for our all-atom simulations by classical molecular dynamics (labeled as with lipid). To assess the impact of PG molecules on the cavity of transmembrane helices core, additional simulation was performed with the two bound PGs (36:2) removed (labeled as no lipid, Supplementary Fig. 1a)." (Lines 629-635).

2. Disulfide Bridge: In chain A of the apo structure (apo_GPR156-model.pdb), there is a disulfide bridge (C191 – C216) that is not present in chain B even though the sulfur atoms are close enough. Can you explain why? Did you consider disulfide bridges during the preparation of the structures for the simulations?

Response: We thank the reviewer for this kindly remind. We have measured the distance between sulfur atoms of C191 and C216 in the apo structure (apo_GPR156-model.pdb), and found that the distance is too large to form the disulfide bridge (Supplementary Fig. 1b). Thus, we have not considered these disulfide bridges in our MD simulations. To address this issue, we have added the following sentence in the Material and Methods section.

"For both simulations, the disulfide bridge between C191 and C216 was not consider due to the large distance (Supplementary Fig. 1b)." (Lines 635-636).

3. Model Construction: It is specified that the membrane model contains POPC and POPE (ratio 3:1) and that 7 CHL molecules are also present. Do these CHL molecules correspond to those initially present in the structure or were they added by CHARMM-GUI?

Response: We thank the reviewer for this important suggestion. To address these issues, we have revised the following sentences in the Material and Methods section.

"From the apo structure of the GPR156 dimer complex, the two transmembrane helix core-bound phospholipids were removed, except the PGs (36:2) and the cholesterol molecule in the interface of GPR156 dimer." (Lines 629-631).

"The resulting system had a total of 240 lipid and 7 cholesterol molecules (added by CHARMM-GUI) in each leaflet and was solvated in a cubic box with TIP3P waters and 0.15 M Na^+/Cl^- ions." (Lines 639-641).

4. System Size: Indicate the dimensions and the number of atoms.

Response: We thank the reviewer for this important suggestion. To address these issues, we have revised the following sentences in the Material and Methods section.

"The system sizes of the GPR156 (with lipid) and the GPR156 (no lipid) were 13.4×13.4×13.1 nm^3, which contained a total number of 223,513, and 223,194 atoms. In addition, the corresponding number of water molecules were 49,631 and 49,612, and the number of ions were 135 Na^+ and 154 Cl^-, and 134 Na^+ and 155 Cl^-, respectively (Supplementary Table 2)." (Lines 641-645).

5. Type of Simulation: Specify that it is an all-atom simulation by classical molecular dynamics.

Response: We thank the reviewer for these important suggestions. To address these issues, we have revised the following sentences in the Material and Methods section.

"The retained GPR156-dimer complex was used as the input conformation for our all-atom simulations by classical molecular dynamics (labeled as with lipid)." (Lines 631-633).

##########

Miscellaneous

##########

1. Line 198: You refer to Ballesteros-Weinstein numbering at this point in the article, but you use this notation earlier in the previous section. Please clarify the use of Ballesteros numbering when you use it for the first time (line 168).

Response: We thank the reviewer for the careful reviewing. We clarify the use of Ballesteros numbering when it first used in our revised manuscript (Lines 169-170).

2. Line 206: You write: "form van der Waals force", which is incorrect. You can simply indicate that residues L237, Y241, and L234 are in contact with residues M261 and N265.

Response: We thank the reviewer for pointing out the mistake. We have rephrased the statement accordingly (Lines 206-208).

3. Lines 253-254: You write: "a comparative analysis between apo GPR156 and the active GPR156 dimer revealed striking similarity (RMSD of 0.494 Å)". However, when I perform this alignment on alpha carbons, I get an RMSD of about 1 Å (apo_GPR156-model.pdb and GPR156_Gi3_complex-model.pdb). Did you consider all the residues of the protein or only part of it (i.e., the transmembrane domain)? Please clarify.

Response: We appreciate the reviewer to point this out. In response, we re-examined our data. When we perform the superposition analysis between apo GPR156 (all residues) and active GPR156 from GPR156-G_{i3} complex (all residues) by using "Matchmarker" function in UCSF Chimera X package, we get the result (RMSD of 0.494 Å for pruned 288aa; RMSD of 0.841 Å for all 298aa) as we reported before, as shown below:

> Matchmaker apo_GPR156-model.pdb, chain B (#1) with GPR156_Gi3_complex-model.pdb, chain B (#2), sequence alignment score = 1556.6
> RMSD between 288 pruned atom pairs is 0.494 angstroms; (across all 298 pairs: 0.841)

But we found that only 298 pairs were used for comparison. After looking at the Chimera X

package manual, we found that this function can only be compared to one chain. Therefore, we made adjustments to compare the dimer as a whole, and the final result (RMSD of 0.539 Å for pruned 572aa; RMSD of 0.902 Å for all 596aa) was consistent with the reviewer's result (an RMSD of about 1 Å), as shown in the figure below:

> Matchmaker apo_GPR156-model-coot-0-TEST-RMSD.pdb, chain A (#1) with GPR156_Gi3_complex-model-coot-0-TEST-RMSD.pdb, chain A (#2), sequence alignment score = 3079.5
> RMSD between 572 pruned atom pairs is 0.539 angstroms; (across all 596 pairs: 0.902)

Thanks again for the reviewer's careful check. We have revised this point in our revised manuscript (Line 255).

4. Figure 2, panel a: The text size of the legend of the phylogenetic tree (ion, orphan, amino acid, and sensory) is too small. I have to zoom in at 160% to read it. Please increase the font size.

Response: We thank the reviewer's helpful suggestion. We have revised Figure 2a for better presentation as shown below:

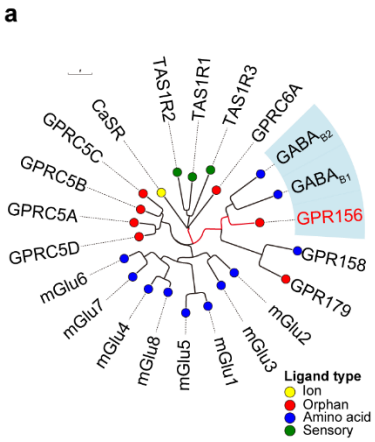

Fig. 2a

5. Figure 4, panel e: The label size is too small as well.

Response: We thank the reviewer's helpful suggestion. We have revised Figure 4e and also other figures which have same problem (Figure 5d; Figure 6f, g, h; Extended Data Fig. 2c) for better presentation as shown below:

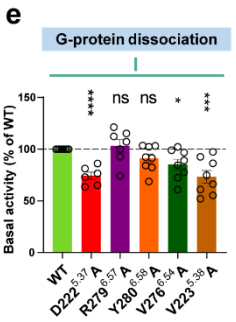

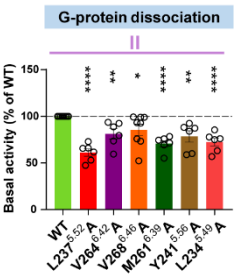

Fig. 4e

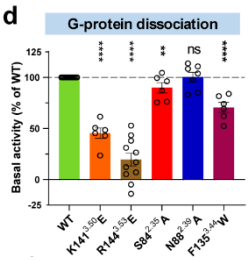

Fig. 5d

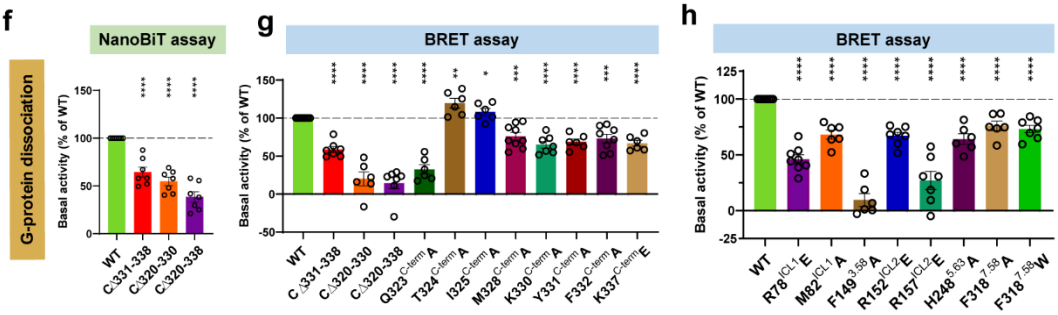

Fig. 6f, g, h

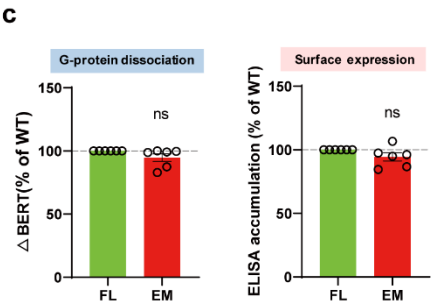

Extended Data Fig. 2c

6. Supplementary Figure 1: I noticed that the authors simulated the GPR156 homodimer with both endogenous ligands (phosphatidylglycerol). However, the duration is only 50 ns (1 replicate). Can you extend the simulations to 300 ns and 3 replicates? If not, it should be mentioned in the Materials and Methods section.

Response: We thank the reviewer for this important suggestion. We agree that the simulation time should be consistent between the GPR156 (no lipid) and the GPR156 (with lipid). We have therefore extended the simulation time of the GPR156 (with lipid) to 300 ns, and revised the following sentences and the corresponding analyses results, as listed below.

"Finally, to escape the uncertainties of the sampling results, three replicates of the production run of 300 ns MD simulation with different initial velocities were performed for both systems: the GPR156 (with lipid) and the GPR156 (no lipid) (Supplementary Fig. 2). …" (Lines 657-660)

The corresponding results in Extended Data Fig. 10h (Extended Data Fig. 13h in prior version) and Supplementary Fig. 2 (Supplementary Fig. 1 in prior version) have also been revised. Meanwhile, we have also revised the term for the phospholipid-free GPR156 in Supplementary Fig. 2 and replaced it with the term "GPR156 (no lipid)".

Response to Reviewer #3:
Reviewer #3:

Here Ma et al. present a significant study on the class C orphan G-protein-coupled receptor (GPCR) GPR156, emphasizing its role in auditory function via Gi2/3 signaling. The work presents the structural insights obtained from cryo-EM studies, which reveal an unconventional extracellular region and a dimerization interface that contributes to GPR156's activity. Furthermore, the authors describe a dual role of the C-terminus in G protein binding, offering mechanistic insights into how GPCR constitutive activity is sustained.

Overall, the work is very well presented, and both the functional and structural experiments are nicely done. While the aim of this research is highly significant, given the limited information available on the structural features of GPR156, the auditory function studies remain incomplete. To enhance the impact and comprehensiveness of this study, several clarifications are necessary.

Response: We thank the Reviewer #3 for the constructive feedback and positive assessment. We have addressed the following points to strengthen our manuscript:

Below are some suggestions:

1) Previous work by Kindt et al. (2021) demonstrated that GPR156 plays a crucial role in the development of the auditory system. In this study, the authors investigate whether GPR156 continues to be important after auditory maturity is reached. To address this, they performed in vivo knock-down experiments using AAV-mediated GPR156-shRNA at three time points: the auditory development stage (P2–P3), the mature auditory stage (P30), and the late stage of auditory maturation (P60).
However, a significant issue is that the virus injections were carried out in the C57 mouse strain, which is known for early-onset hearing loss due to the Ahl allele, causing progressive hearing loss starting as early as 3 months of age. While the final time point in the study is P75, which is just under this threshold, it still presents potential challenges for interpreting the results. Both the downregulation of GPR156 and the mutation in cadherin 23 could contribute to the observed effects. The authors should address this limitation in their manuscript, discussing the implications of using the C57 strain for long-term auditory studies.
Response: Thank you for your suggestions. In our work, we delivered AAV-7m8-GPR156-shRNA in the left ear of the mice and used the right ear as the control before, and now further broadened our control groups to include both uninjected mice (WT mice) and mice injected with control viruses. We found no significant difference in hearing thresholds among the right ear, WT mice, and mice injected with control viruses, and the choice of the right ear as the control group could minimize the problem of age-related hearing loss in C57 strain mice (as shown in the response to the next point, which also shown in Fig. 1c, h).

2) To ensure robust interpretation of the auditory function tests, it is essential to include both uninjected mice and mice injected with a control virus. These controls are particularly important given the use of the C57 strain, which has a predisposition for early-onset hearing loss. The authors only include ABR recordings from the contralateral ear as control. However, it is well-established that a virus injected in one ear can also affect hearing in the opposite ear."

Response: Thank you for your suggestions. According to your advice, we have added ABR results from the un-injected mice and mice injected with a control virus in the revised manuscript, as listed below.

"Of particular interest is the observation that upon maturation of the auditory faculty (P30 and P60) knockdown of GPR156 leads to severe hearing loss (Fig. 1c-q)," (Lines 122-124)

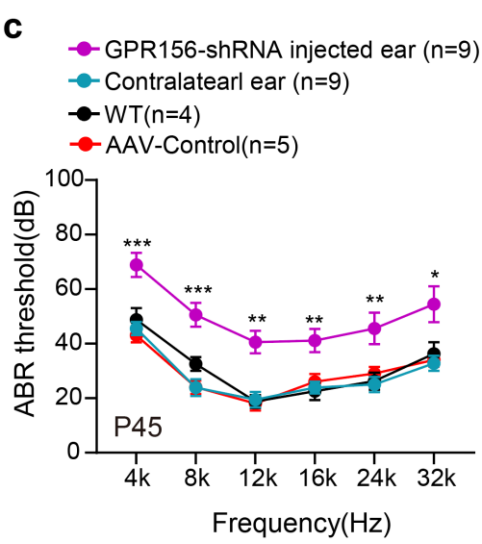

Fig. 1c

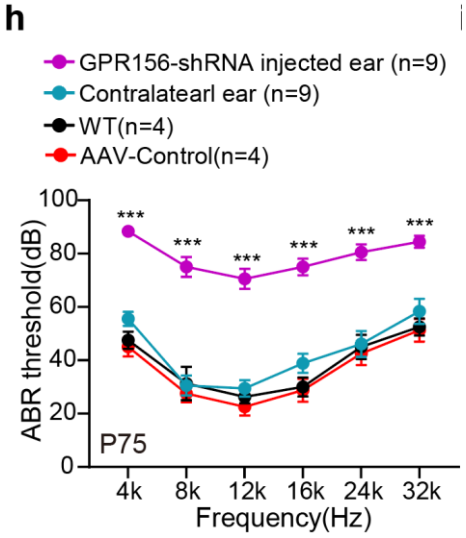

Fig. 1h

3) In Figure 1, the authors show that both the P30 (Fig. 1a) and P60 (Fig. 1h) injections result in nearly 40% hair cell loss, although they do not distinguish between inner hair cells (IHCs) and outer hair cells (OHCs). It is intriguing that despite similar hair cell loss percentages, the P30 injection leads to a 10-20 dB SPL threshold elevation, while the P60 injection results in a 10-50 dB SPL elevation (Figs 1c and 1i). Additionally, given the significant hair cell loss observed in the representative immunofluorescence images, especially IHC loss in the cochlear base (Figs. 1e and 1k), it is surprising to see only a small ABR threshold elevation in the high-frequency region.

Therefore, it is important to count IHCs and OHCs separately. Furthermore, to assess the contribution of GPR156 to OHC function, it would be informative to include DPOAE recordings. The discrepancy in threshold elevations (Figs 1c and 1i) should be further analyzed and better explained.

Response: Thank you for your suggestions. According to your advice, we added the statistics of IHC and OHC, as listed below (Fig. 1g, l in the revised manuscript). Based on the statistics, we found that compared with P30 mice injected with AAV-GPR156-shRNA, P60 mice showed more impairment of IHC and Ctbp2(Fig. 1n-q in the revised manuscript), which may be due to the fact that the knockdown of GPR156 is more sensitive to the hair cells of P60.

"Of particular interest is the observation that upon maturation of the auditory faculty (P30 and P60) knockdown of GPR156 leads to severe hearing loss (Fig. 1c-q), partial loss of HCs and synapses (Fig. 1d, e, g, i, j, l, n, o, p, q)." (Lines 122-125)

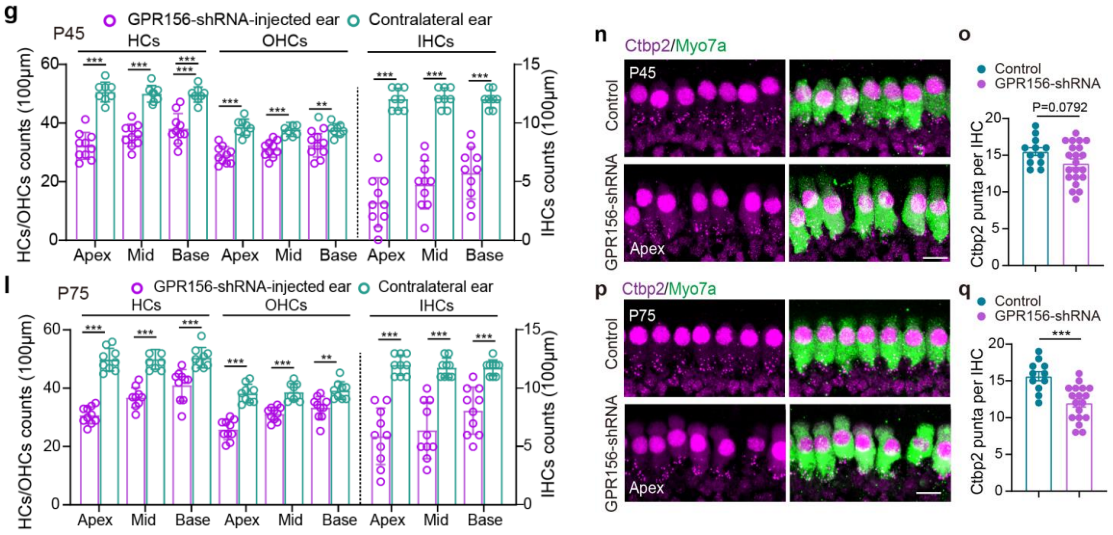

Fig. 1g, l Fig. 1n-q

Relevant to evaluating the contribution of GPR156 to OHC function: GPR156 was knocked down by delivering AAV-7m8-GPR156-shRNA. AAV-7m8 is one of the AAVs with high efficiency in infecting HCs in neonatal mice, but it cannot infect 100% of the OHCs in adult mice (Isgrig et al., 2019). And up to now, there is no AAV that can infect 100% of the HCs in adult mice (Isgrig et al., 2019; Gyorgy et al., 2019; Tan et al., 2019). Considering the limitations of AAV transfection of adult mouse HCs and the age of mice, it is not suitable to explore the effect of GPR156 on OHC function and DPOAE with the AAV-7m8 in detail. Therefore, we have obtained $GPR156^{loxp/loxp}$ and GPR156-KO mice and will utilize them to fully investigate the effect of GPR156 on auditory function and OHC function in the future.

We thank again the reviewer for pointing this out. And we have stated the limitations of this point in Discussion part of our revised manuscript, as listed below.

"Since there is no AAV that can efficiently infect the OHCs of adult mice[38-40], and the limitation of age-related hearing loss in C57 strain mice[41], in order to further investigate the effects of GPR156 on hearing function and its mechanism of action at different time points, subsequent studies using new AAV vectors or transgenic mice are needed." (Lines 420-424)

Reference:

Isgrig, K. et al. AAV2.7m8 is a powerful viral vector for inner ear gene therapy. Nat Commun 10, 427 (2019).

Gyorgy, B. et al. Gene Transfer with AAV9-PHP.B Rescues Hearing in a Mouse Model of Usher Syndrome 3A and Transduces Hair Cells in a Non-human Primate. Mol Ther Methods Clin Dev 13, 1-13 (2019).

Tan, F. et al. AAV-ie enables safe and efficient gene transfer to inner ear cells. Nat Commun 10, 3733 (2019).

4) It is important to conduct immunohistochemistry assays using antibodies against GPR156 to quantify the reduction of the protein in hair cells and compare these results with the

relative mRNA expression levels in the cochlea.

Response: Thank you for your suggestions. According to previous studies, GPR156 is mainly expressed in inner ear hair cells (Kindt et al., 2021). We purchased three GPR156 antibodies that are currently available on the market. We first tested the GPR156 antibody in P1 wild-type mice. The antibody from Novus (NBP1-83402) was not specific for hair cells, and the antibodies from Affinity (DF4955) and Thermofisher (PA5-102090) labeled the hair cells; however, neither of these two antibodies were good for OHC infections in adult mice. We utilized Thermofisher 's antibody to detect GPR156 expression in the follow-up experiment, using the same intensity of fluorescence to photograph the GPR156 fluorescence channel, and although OHC staining results were poor, the fluorescence intensity of GPR156 in the remaining IHCs after P30 and P60 injections of AAV-GPR156-shRNA was significantly lower than that in the control group. Similarly, RT-qPCR results showed the same trend of decreased relative mRNA expression of GPR156. Although the specificity of the GPR156 antibody was poor, overall, these results could show a decrease in GPR156 expression. And these details are shown below.

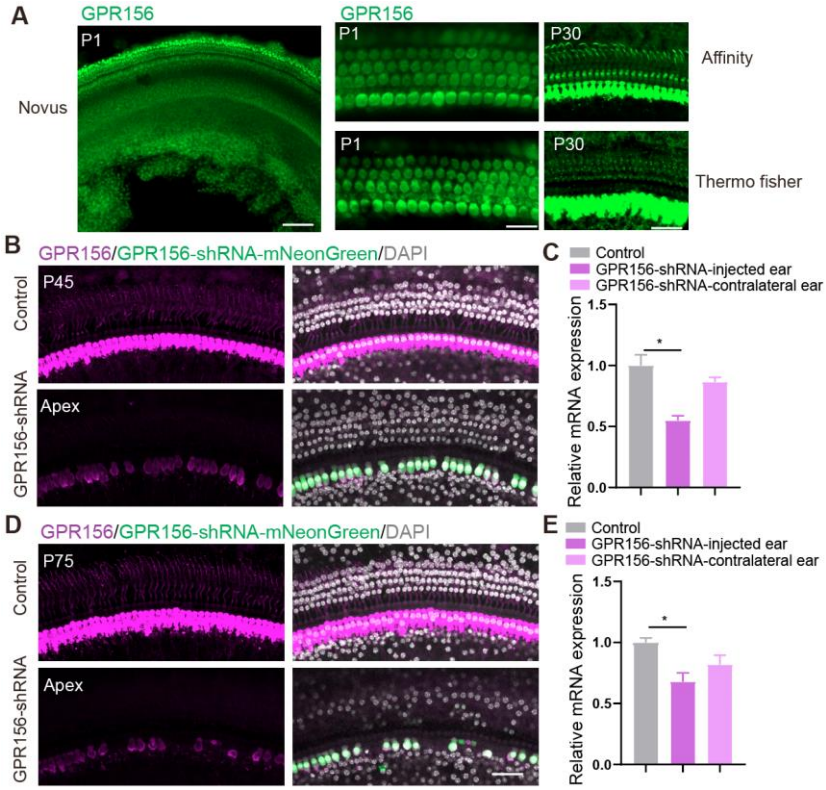

A: The images of GPR156 staining in P1 and P30 mice. GPR156: green. Scale bar: 200um, 80um.

B: The images of GPR156 staining in AAV-GPR156-shRNA transduced P45 mice. GPR156: magenta. AAV-GPR156-shRNA: green. DAPI: gray. Scale bar: 40um.

C: The transcriptome expression level of GPR156 in AAV-GPR156-shRNA transduced P45 mice.

D: The images of GPR156 staining in AAV-GPR156-shRNA transduced P75 mice. GPR156: magenta. AAV-GPR156-shRNA: green. DAPI: gray. Scale bar: 40um.

E: The transcriptome expression level of GPR156 in AAV-GPR156-shRNA transduced P75 mice.

Reference:

Kindt, K.S. et al. EMX2-GPR156-Gαi reverses hair cell orientation in mechanosensory epithelia. Nat Commun 12, 2861 (2021).

5) To strengthen the significance of GPR156 knockdown on auditory function, it is important to analyze the state of auditory innervation (afferent and efferent synapses) to the organ of Corti, as well as the condition of hair cell stereocilia. This can be accomplished through high-resolution immunofluorescence using well-described specific antibodies and subsequent analysis with a high-resolution confocal microscope.

Response: Thank you for your suggestions. According to previous studies, we examined the presynaptic marker Ctbp2, and the statistical results showed that injection of AAV-GPR156-shRNA at P30 had almost no effect on Ctbp2, whereas injection of AAV-GPR156-shRNA at P60 resulted in a slight decrease in Ctbp2. This may also account for the greater effect of AAV-GPR156-shRNA on mouse hearing at P60. And these details are shown below.

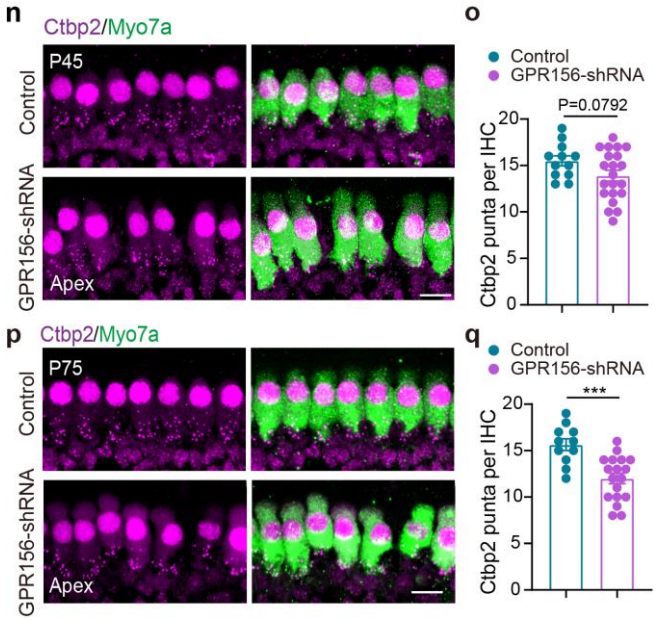

Fig. 1n-q

And, we analyzed the morphology of hair cell stereocilia, and the image results showed that the stereocilia of P30 and P60 injected with AAV-GPR156-shRNA appeared significantly disorganized, as shown below.

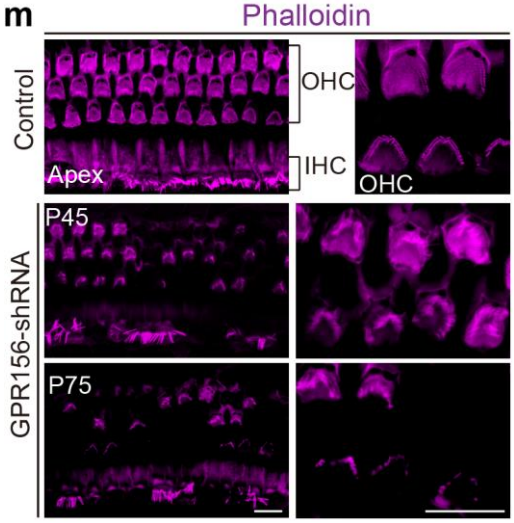

Fig. 1m

"Of particular interest is the observation that upon maturation of the auditory faculty (P30 and P60) knockdown of GPR156 leads to severe hearing loss (Fig. 1c-q), partial loss of HCs and synapses (Fig. 1d, e, g, i, j, l, n, o, p, q)." (Lines 122-125)

6) In the present manuscript, the authors conduct an elegant study investigating the cryo-EM structures of human apo GPR156 and the GPR156–Gi3 complex, elucidating the structural features of the complex. The study is noteworthy for its thorough examination of the unique N-terminus, as well as the structural details of both the transmembrane domain (TMD) and C-terminus. Additionally, the authors assess basal activity through constructs with mutations in the C-terminal tail to analyze its interaction with the TMD of GPR156 and Gαi. However, the way it is written, avoiding explaining with details the performed experiments, coupled with the big amount of extended figures makes it difficult to follow. Simplifying the presentation of supplementary data and providing clearer explanations of the figures would enhance the readability and understanding of the study.

Response: We thank the reviewer's valuable suggestion. In response to your recommendations, we make the following changes:

1) We have added the details of performed experiments include the information about two kinds of AAV-mediated GPR156-shRNAs (as also mentioned by reviewer #1), the description of statistical methods for the in vivo experiment related to mice (as also mentioned by reviewer #1), the details of Fig. 5f and Extended Data Fig. 9c (previously Extended Data Fig. 12c) (as also mentioned by reviewer #1), and more MD protocol details (as also mentioned by reviewer #2).

   And these details are shown below.

   The information about two kinds of AAV-mediated GPR156-shRNAs:

   "The sense strand sequence of GPR156-shRNA1 and GPR156-shRNA2 were cgg agc atg caa tgt agc ttt and gta ccg ttt cta gtt cac aaa, respectively. And the loop sequence of GPR156-shRNA was tcaagag." (Lines 445-447)

   The description of statistical methods for the in vivo experiment related to mice:

   "Bar graphs depict the differences of each mutant relative to the WT receptor or contralateral ear/WT mice. *In vitro* data were from at least six independent experiments, each conducted in triplicate. *In vivo* experiments related to mice were repeated at least three times. $*P < 0.05$, $**P < 0.01$, $***P < 0.001$, $****P < 0.0001$ (two-tailed unpaired t test for all data)." (Lines 710-714)

   The details of Fig. 5f and Extended Data Fig. 9c (previously Extended Data Fig. 12c):

   "Figure 5f, Upon G protein coupling, the dimeric TMD of five class C GPCRs (including $mGlu3_{free}$–$mGlu2_{G}$ (Cα of V699; PDB code: 8JD3), $mGlu4_{free}$–$mGlu2_{G}$ (Cα of V699; PDB code: 8JD5), $mGlu2_{free}$–$mGlu2_{G}$ (Cα of V769; PDB code: 7MTS), $CaSR_{free}$–$CaSR_{G}$ (Cα of M771; PDB code: 8WPU), and $GABA_{B1(free)}$–$GABA_{B2(G)}$ (Cα of C614; PDB code: 7EB2)) undergo conformational rearrangements, except for $GPR156_{free}$–$GPR156_{G}$." in Lines 1021-1026.

   "Extended Data Fig. 9b, c, Statistical analysis of the dimeric interface area (**b**) and the

distance (**c**) of class C GPCR dimers with the G protein (including $GPR156_{free}$–$GPR156_G$ (Cα of G244-G244), $CaSR_{free}$–$CaSR_G$ (Cα of T828-A824; PDB code: 8WPU), $mGlu4_{free}$–$mGlu4_G$ (Cα of I804-I804; PDB code: 7E9H), $mGlu4_{free}$–$mGlu2_G$ (Cα of T808-V782; PDB code: 8JD5), $mGlu3_{free}$–$mGlu2_G$ (Cα of T792-V782; PDB code: 8JD3), $mGlu2_{free}$–$mGlu2_G$ (Cα of T783-V782; PDB code: 7MTS), and $GABA_{B1(free)}$–$GABA_{B2(G)}$ (Cα of A832-L712; PDB code: 7EB2))." in Lines 1165-1171.

More MD protocol details:

"From the apo structure of the GPR156 dimer complex, the two transmembrane helix core-bound phospholipids were removed, except the PGs (36:2) and the cholesterol molecule in the interface of GPR156 dimer. The retained GPR156-dimer complex was used as the input conformation for our all-atom simulations by classical molecular dynamics (labeled as with lipid). To assess the impact of PG molecules on the cavity of transmembrane helices core, additional simulation was performed with the two bound PGs (36:2) removed (labeled as no lipid, Supplementary Fig. 1a). For both simulations, the disulfide bridge between C191 and C216 was not consider due to the large distance (Supplementary Fig. 1b)." (Lines 629-636).

"The resulting system had a total of 240 lipid and 7 cholesterol molecules (added by CHARMM-GUI) in each leaflet and was solvated in a cubic box with TIP3P waters and 0.15 M Na^+/Cl^- ions. The system sizes of the GPR156 (with lipid) and the GPR156 (no lipid) were 13.4×13.4×13.1 nm^3, which contained a total number of 223,513, and 223,194 atoms. In addition, the corresponding number of water molecules were 49,631 and 49,612, and the number of ions were 135 Na^+ and 154 Cl^-, and 134 Na^+ and 155 Cl^-, respectively (Supplementary Table 2)." (Lines 639-645).

"After 5000 steps of energy minimization performed by the steepest descent algorithm, a 250 ps NVT equilibration simulation was performed at 310 K, with the default restraint potential ($k_{BC/SD/LIP/DIH}$=10.0/5.0/2.5/2.5 $kcal{\cdot}mol^{-1}{\cdot}Å^{-2}$) on the heavy atoms of backbone, sidechain, lipid and dihedral angle. Subsequently, a cumulatively 1.65 ns NPT equilibration to 1 atm was performed using the Berendsen barostat[62], with the restraint potential gradually reduced to zero." (Lines 647-652).

"During the pre-equilibrium simulation, the vacuum of the cavities of the transmembrane helices core for the GPR156 (no lipid) system was gradually filled with water molecules (Supplementary Fig. 1c). Finally, to escape the uncertainties of the sampling results, three replicates of the production run of 300 ns MD simulation with different initial velocities were performed for both systems: the GPR156 (with lipid) and the GPR156 (no lipid) (Supplementary Fig. 2). …" (Lines 655-660).

"The RMSD of the transmembrane helices (TM3/5/6/7) ends (heavy atoms of 10 residues) in the intracellular side were calculated, and other C alpha atoms of the transmembrane helices were used for structural alignment (Supplementary Figs. 3-6; Supplementary Table 3). For the RMSD calculation, the first 10 ns was ignored and only the last 290 ns MD simulation data was used. GROMACS's rms function was used to calculate RMSD." (Lines 663-668).

2) We deleted two redundant Extended Data Figs (the deletion does not affect the understanding of the content of the manuscript), including previously Extended Data Fig. 6 and previously Extended Data Fig. 11.

3) We deleted previously Extended Data Fig. 9d, e (the deletion does not affect the understanding of the content of the manuscript), and integrated previously Extended Data Fig. 9 (except for d and e) and previously Extended Data Fig. 10 into a single picture Extended Data Fig. 8 of our revised manuscript.

4) We also revised the figure legends of Figure 2 and Extended Data Figs. 2, 3, 4, 5. And these details are shown below：

"Figure 2c, The structural features of class C GPCRs include mGluR or CaSR (purple), GPR158 or GPR179 (green), GB1 subunit (orange), GB2 subunit (yellow), and GPR156 (blue). **d, e,** Cryo-EM maps (left panel) and models (right panel) of human apo GPR156 (**d**) and GPR156–G_{i3} complex (**e**)." in Lines 965-968.

"Extended Data Fig. 2c, Basal activity (left panel) and surface expression (right panel) of the FL and EM constructs of GPR156, as measured by BRET-based assay and ELISA assay, respectively." and **"d, e,** Size-exclusion chromatography profile (left panel), SDS–PAGE gel (middle panel), and western blot (right panel) of the purified apo GPR156 (**d**) and GPR156–G_{i3} complex (**e**)." in Lines 1073-1074 and 1079-1081.

"Extended Data Fig. 3a, Representative cryo-EM micrograph (top panel) and 2D averages (bottom panel) for apo GPR156." in Lines 1085-1086.

"Extended Data Fig. 4a, Representative cryo-EM micrograph (top panel) and 2D averages (bottom panel) for the GPR156–G_{i3} complex." in Lines 1096-1097.

"Extended Data Fig. 5c, d, Cryo-EM density and the fitted atomic model of the GPR156–G_{i3} complex, including N-terminus, transmembrane helices, ECLs, ICLs, PG 36:2 of the GPR156 G-free subunit (**c**), N-terminus, transmembrane helices, ECLs, ICLs, CLR, PG 36:2, C-terminus of the GPR156 G-bound subunit, and the α5 helix of $G\alpha_{i3}$ (**d**)." in Lines 1109-1112.

Reviewer #2 attachment:

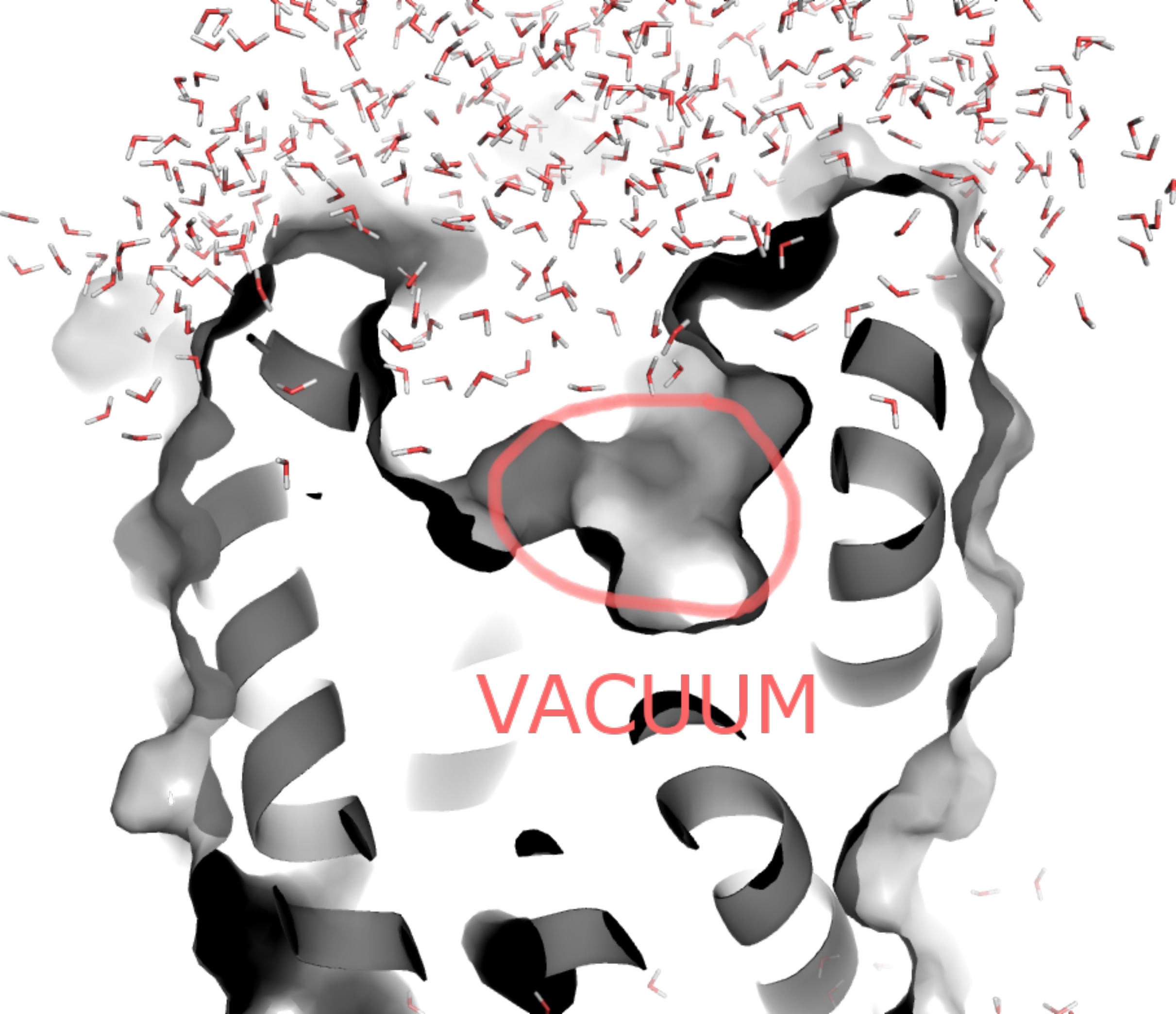
VACUUM